Oral exposure to cadmium and mercury alone and in combination causes damage to the lung tissue of Sprague-Dawley rats

Sirasha Venketsamy Koopsamy Naidoo[1], Megan Jean Bester[1], Sandra Arbi[1], Chantelle Venter[2] Priyanka Dhanraj[1], Hester Magdalena Oberholzer[1,*]

[1]Department of Anatomy, Faculty of Health Sciences, University of Pretoria, Private Bag x323, Arcadia, 0007, South Africa
[2] Laboratory for Microscopy and Microanalysis, University of Pretoria

*Corresponding author:
Prof HM Oberholzer
Department of Anatomy,
Faculty of Health Sciences
University of Pretoria
Private Bag x323
Arcadia, 0007
South Africa

Highlights

- Oral exposure to cadmium and mercury causes changes to the lung architecture.
- Changes in bronchiole morphology included an increase in smooth muscle mass.
- Luminal epithelium degeneration, detachment and aggregation.
- Prominent bronchiole-associated lymphoid tissue was present in Cd and Hg.
- Ultrastructural examination confirmed the presence of fibrosis.

Abstract

Environmental presence and human exposure to heavy metals in air and cigarette smoke has led to a worldwide increase in respiratory disease. The effects of oral exposure to heavy metals in liver and kidney structure and function have been widely investigated and the respiratory system as a target is often overlooked. The aim of the study was to investigate the possible structural changes in the lung tissue of Sprague-Dawley rats after oral exposure for 28 days to cadmium (Cd) and mercury (Hg), alone and in combination at 1000 times the World Health Organization's limit for each metal in drinking water. Following exposure, the general morphology of the bronchiole and lungs as well as collagen and elastin distribution was evaluated using histological techniques and transmission electron microscopy. In the lungs, structural changes to the alveoli included collapsed alveolar spaces, presence of inflammatory cells and thickening of the alveolar walls. In addition, exposure to Cd and Hg caused degeneration of the alveolar structures resulting in confluent alveoli. Changes in bronchiole morphology included an increase in smooth muscle mass with luminal epithelium degeneration, detachment and aggregation. Prominent bronchiole-associated lymphoid tissue was present in the group exposed to Cd and Hg. Ultrastructural examination confirmed the presence of fibrosis where in the Cd exposed group, collagen fibrils arrangement was dense, while in the Hg exposed group, additional prominent elastin was present. This study identified the lungs as target of heavy metals toxicity following oral exposure resulting in cellular damage, inflammation and fibrosis and increased risk of respiratory disease where Hg showed the greatest fibrotic effect, which was further, aggravated in combination with Cd.

Key words: Heavy metals; cadmium; mercury; reactive oxygen species; lungs; toxicity.

1. Introduction

The main source of heavy metal exposure is through the anthropogenic sources such as transport, agriculture, mining and other related operations (Venter *et al.,* 2017). Established routes of exposure are absorption through the skin, oral cavity and via inhalation (Awofolu *et al*., 2005). Air pollution is the most common cause of respiratory disease that affects the structure and the functioning of the airways and the respiratory components of the lungs. The most common respiratory diseases associated with exposure are asthma, bronchitis, chronic cough, chronic obstructive pulmonary disease (COPD), idiopathic pulmonary fibrosis, lung cancer, pneumonia and tuberculosis. The World Health Organization (WHO) (2000) reported an increase in the prevalence of respiratory diseases from 100 to 400 million from 2006 to 2010 (Mamuya *et al*., 2007).

Exposure is often not limited to a single metal and depends on the type of mining; the method of extraction, the degree to which safety measures are implemented as well as other activities such as cigarette smoking that can result in exposure to several components at different concentrations. Incorrect disposal of heavy metals may also result in the leaching of waste into various water sources and thus polluting the water (McCarthy, 2011). The United States Environmental Protective Agency (EPA) in 2013 analysed municipal water supplies for the following heavy metal concentrations; aluminium (Al), copper (Cu), arsenic (As), mercury (Hg) and lead (Pb). Luo *et al*., (2011) showed a high concentration of cadmium (Cd), Pb, and nickel (Ni) exceeding the limit of 1000 ppm and suggested that industrial contaminants have leached into the municipality water supply. Studies in South Africa examined and reported elevated levels of heavy metals in the drinking water near a mining industry in the Witwatersrand region (Naicker *et al*., 2003). This water is used for drinking, washing and recreational purposes. Exposure to heavy metals are found to have numerous detrimental effects on human health. According to Rehman *et al.,* (2018), constant exposure to heavy metals often leads to the accumulation of heavy metals in various parts of the body. Accumulated heavy metals may interfere or alter the functioning of essential molecules such as carbohydrates, proteins and lipids through the induction of oxidative stress. As a result, numerous metabolic processes and mechanisms are affected. This is often followed by a cascade of detrimental effects including neuronal damage, cardiovascular disorders, kidney and liver damage and several types of cancers (Rehman *et al.,* 2018).

The effects of metals such as Hg and Cd on the liver and kidneys, common organs of toxicity, has been widely investigated in several animal models (Jarup, 2003; Leem *et al.,* 2015). However, little is known regarding oral absorption on lung function. Workers in primary metal industries are also at a risk of exposure, as Cd is a pulmonary irritant and fatal when inhaled

(Nawrot *et al*., 2010). Increased blood levels of Cd is associated with a decrease in pulmonary function (Bertin and Averbeck, 2006; Huff *et al.,* 2007; Nawrot *et al.,* 2010). Hg is toxic to humans and causes severe alterations such as DNA mutation that activates oncogenesis, resulting in the transformation of normal cells into tumour cells (Onyido *et al.,* 2004). Previous studies indicated that both the inorganic and organic form of Hg accumulates over a period of time in the endocrine organs (e.g. pituitary gland and hypothalamus) (Zhu *et al*., 2014; Martin and Griswold, 2009). Little is known regarding the effect of metals such as Cd and Hg that are often part of mixtures, where the observed effect would be a function of concentration, exposure time as well as the unique tissue, cellular and biochemical targeting of each metal.

As Cd and Hg are common contaminants of water, the aim of this study was to investigate the morphological changes in the lung tissue and the presence of fibrosis in male Sprague-Dawley rats after oral exposure to relevant dosages of Cd and Hg, alone and in combination. The rationale for using 1000x the acceptable exposure limits as established by the WHO, for a short period of time, is to identify specific cellular targets that can later be further evaluated in chronic models of exposure. Also, the lungs are often overlooked when the toxicity of heavy metals after oral exposure is being investigated and therefore this study aimed to determine whether oral exposure to heavy metals can also contribute to lung damage.

2. Materials and Methods

2.1 Implementation of the Sprague-Dawley rat model

Forty-eight male Sprague-Dawley rats (250 – 300 g) were used in this study and maintained at the University of Pretoria's Biomedical Research Centre (UPBRC). These rats were provided with irradiated commercial Epol rat pellets and water *ad libitum*. All experimental protocols complied with the requirements of the University of Pretoria's Animal Ethics Committee (ethical clearance number: H004-17). The animals were housed in conventional cages complying with the sizes laid out in the SANS 10386:2008 recommendations. A room temperature of 22°C (± 2°C); relative humidity of 50% (± 20%) and a 12-hour light/dark cycle were maintained during the entire study. The rats were allowed to acclimatise for seven days prior to the start of the experiment, which was conducted over the following 28 days. The rats were randomly divided into 4 groups of 6 rats per group and the groups were control, Cd, Hg and Cd+Hg.

2.2 Administration of heavy metals

Cadmium chloride ($CdCl_2$) [Merck (Pty) Ltd, South Africa] and mercury chloride ($HgCl_2$) [Merck (Pty) Ltd, South Africa] were dissolved in sterile water and administered daily to the rats via oral gavage. The control group received saline via oral gavage. Weekly dosages were

adjusted based on the changes in the mass of the rats. The dosage given to the rats was calculated from the WHO water limits for consumption by 60 kg human consuming 1.4 L water per day. The conversion of human dosages to rat dosages was calculated according to the method of Reagan-Shaw *et al.* (2008) and represented a rat equivalent dosage of ± 1000 times the WHO limits in drinking water for human consumption. Dosages were 0.696 mg/kg/day and 1.148 mg/kg/day for rats exposed to Cd and Hg respectively while rats in the Cd + Hg received 0.696 mg/kg and 1.148 mg/kg Cd and Hg respectively.

2.3 Termination

The rats were terminated after 28 days exposure via isoflurane overdose, according to standard methods employed by the UPBRC. Lung tissue was harvested for morphological and ultrastructural analyses.

2.4 Light microscopy

The lung tissue was fixed in 2.5% glutaraldehyde (GA) / formaldehyde (FA), washed with phosphate buffer (pH 7.4) and dehydrated in ascending ethanol concentrations. The tissue was then infiltrated and embedded with paraffin wax. Sections of 3 – 5 µm were made with a Leica RM 2255 wax microtome (Leica Microsystems, Wetzlar, Germany). The slides were then stained with Haematoxylin and Eosin (H&E), Picro-Sirius red and Verhoeff van Geison to evaluate general morphology, collagen and elastin distribution, respectively.

2.5 H&E staining

The slides were placed in xylene for 10 minutes. The sections were rehydrated in a series of decreasing concentrations of EtOH; two changes of 100% EtOH, 90% and 70% each for 1 minute. The slides were then placed in ddH_2O for 1 minute, haematoxylin for 15 minutes and Scott's buffer for 8 minutes. The slides were then rinsed with ddH_2O and then dipped in eosin, 70% EtOH, 90% EtOH, 100% EtOH and xylene. The coverslips were mounted with Entellan® mounting medium. The sections were viewed using a Zeiss AXIO Imager.M2 light microscope (Carl Zeiss Microscopy, Munich, Germany).

2.6 Picro-Sirius Red staining

Picro-Sirius red (PR) staining was performed in order to evaluate and differentiate between collagen fibre types. PR stains collagen and with polarised light microscopy, the collagen fibres are birefringent due to their molecular arrangement (Borges *et al.,* 2007). Thin fibres are viewed as yellow – green birefringence are usually associated with collagen type III while thick fibres appear yellow-orange to orange-red colours and usually consist of type I collagen that have stronger birefringence with polarised light (Velindala *et al*., 2014). To prepare the PR

stain, 0.5 g Sirius red dye was dissolved in 500 ml of aqueous solution of picric acid. Acidified water was used for washing. The tissue was dewaxed and rehydrated, followed by staining in haematoxylin for 8 minutes and rinsed in running tap water for 10 minutes. The tissue was placed in the PR solution for one hour and then washed twice with acidified water. The tissue was then dehydrated three times in 100% ethanol and cleared in xylene. The samples were visualised with a Zeiss AXIO Imager.M2 light microscope (Carl Zeiss Microscopy, Munich, Germany) with a polarising filter.

2.7 Verhoeff van Geison stain

For the Verhoeff van Geison (VvG) stain, 5% alcoholic haematoxylin was prepared with 5 g of haematoxylin dissolved in 100 ml of 100% ethanol. A 10% aqueous ferric chloride solution was prepared with 10 g of ferric chloride dissolved in 100 ml of distilled water. The Weigert's iodine solution consisted of, 2 g of potassium iodide and 1 g of iodine dissolved in 100 ml of distilled water. The VvG working solution was prepared by mixing together 20 ml of 5% alcoholic haematoxylin, 8 ml of ferric chloride and 8 ml of Weigert' iodine solutions. The tissue was deparaffinised and hydrated in distilled water followed by staining with VvG solution for an hour. The tissue was then rinsed with tap water for 6 seconds and was then differentiated using a 2% of ferric chloride solution for 6 seconds. The tissue sections were again rinsed with distilled water and were then treated with 5% of aqueous sodium thiosulfate for 1 minute, followed with another distilled water rinse and Van Gieson counterstain solution for 6 seconds. Dehydration of the tissue sections was performed with 95% ethanol, two rinses of 100% ethanol and finally cleared in two rinses of xylene. The samples were visualised with a Zeiss AXIO Imager.M2 light microscope (Carl Zeiss Microscopy, Munich, Germany).

2.8 Transmission electron microscopy

The tissue samples were fixed in 2.5% GA/FA, washed three times in 0.075 M sodium phosphate buffer (pH 7.4) and then placed in the secondary fixative (1% osmium tetroxide) solution for one hour. Following secondary fixation, the samples were rinsed again as described above. The samples were then dehydrated in 30%, 50%, 70%, 90% and three changes of 100% ethanol and were embedded in epoxy resin. Ultra-thin sections (70 – 100 nm) were cut with a diamond knife using an ultramicrotome. Samples were then contrasted with uranyl acetate and lead citrate, and examined with a JEOL transmission electron microscope (TEM) (JEM 2100F, Tokyo, Japan).

3. Results

Figure 1 is a comparison of the general structure and arrangement of the alveoli between the control (Figure 1 A) and experimental groups (Figure 1 B - D). In Figure 1 A, well defined alveolar spaces (A) can be seen with thin epithelial walls, fine interstitium (asterix) and along the alveolar wall are capillaries containing red blood cells (RBC), all forming the air-blood barrier and respiratory membrane. Pneumocyte type I (P1) and II (P2) can also be identified in the interstitium of alveolar walls. Figure 1 B - D is representative of the lung tissue of Sprague-Dawley rats exposed to the heavy metals alone and in combination (Cd, Hg and Cd + Hg). Figure 1 B and C are representative of the Cd and Hg single metal exposure groups respectively and Figure 1 D is representative of the combination group. In all metal exposed groups, a thickened inter-alveolar space (dashed arrow) is present with increased prominence of the interstitial connective tissue (arrows) and cell nuclei. The presence of RBC is more pronounced along the alveolar wall and surrounding the alveolar spaces in the exposed groups compared to the control and is most obvious in the single metal exposed groups (Figure 1 B and C).

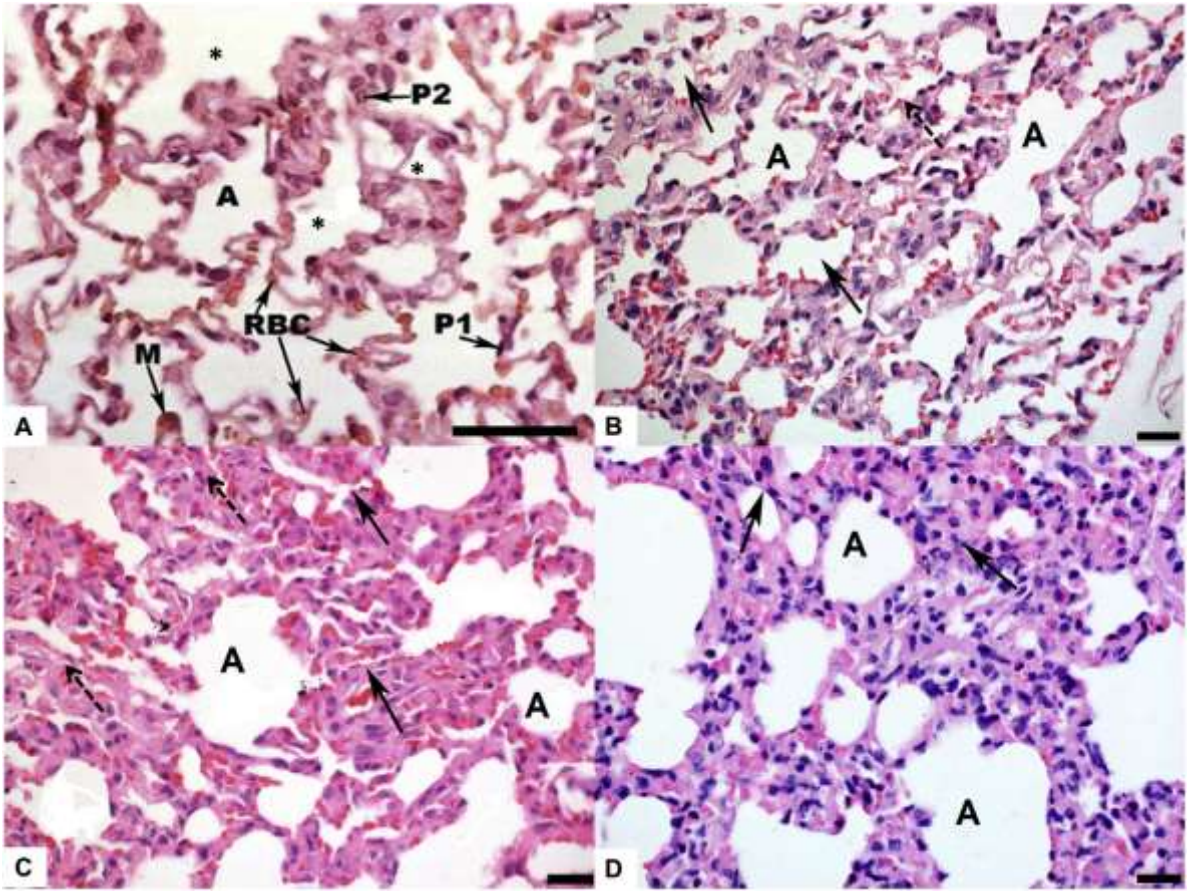

Figure 1: General structure of the lung alveoli and interalveolar wall. H & E staining. A: Control; B: Cd; C: Hg; D: Cd + Hg. Labels: A: alveolar spaces; P1: Type I pneumocyte; P2: type II pneumocyte; RBC: red blood cells; M: alveolar macrophage. Asterix: fine interstitium; Arrow: thick interstitium; Dashed arrow: collapsed alveolar space (Scale bar in A = 50 µm and B - D = 20 µm).

Figure 2 shows the collagen distribution within the alveoli in the control (Figure 2 A) and experimental groups (Figure 2 B - D). In Figure 2 A, predominantly yellow – green birefringence is present in the connective tissue of the interstitium indicative of collagen type III fibres. Slight orange – red birefringence is shown with arrows and is indicative of collagen type I fibres. The Cd exposed group (Figure 2 B) showed some increased orange-red birefringence (collagen type I) when compared to control, indicated with arrows. The Hg exposed group (Figure 2 C) showed primarily orange-red birefringent collagen in the alveoli, which is a strong representation of collagen type I presence and fibrotic tissue. The Cd + Hg exposed group (Figure 2 D) also had an increase of collagen type I in comparison to control, as evident with the orange – red birefringent collagen (arrows) and is similar to that observed in the Cd exposed group.

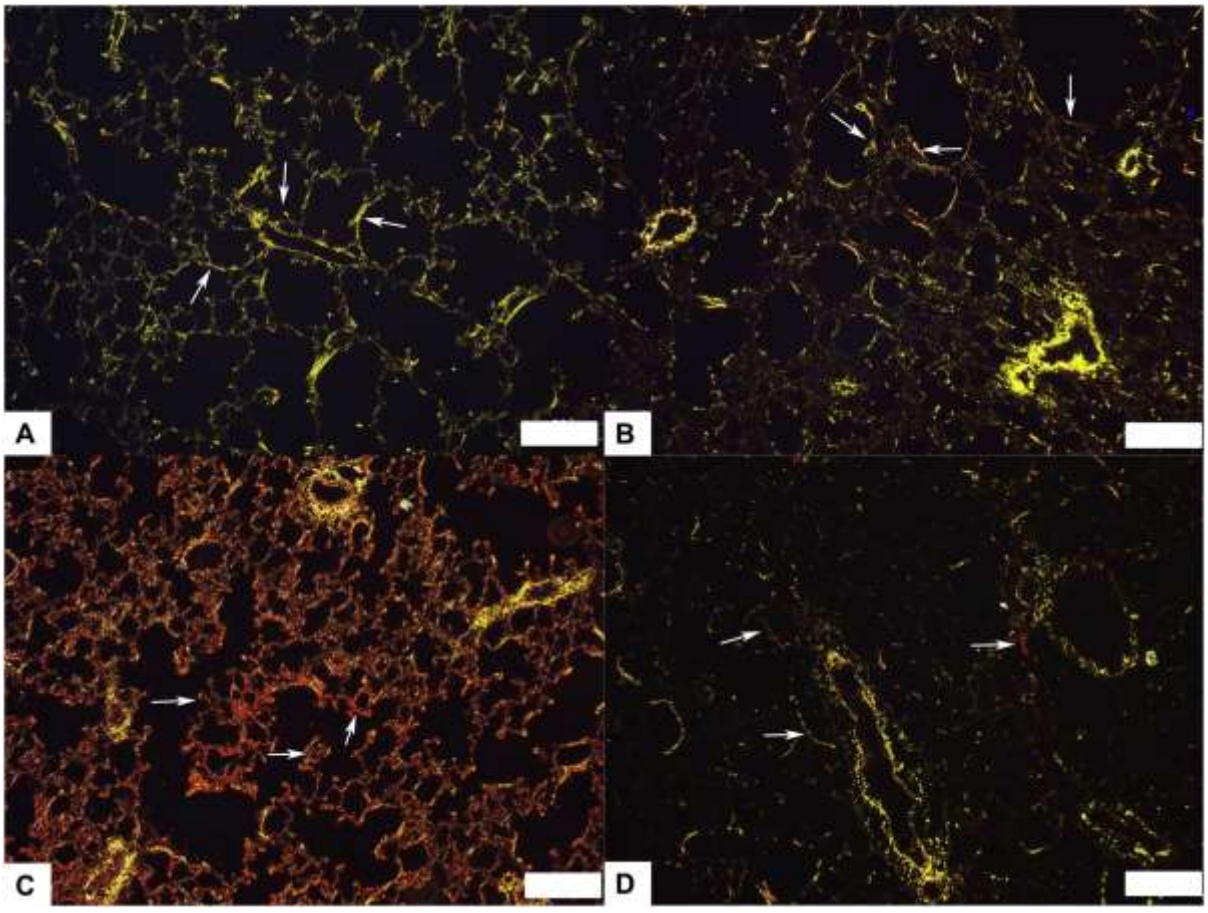

Figure 2: Collagen distribution in the alveoli. PR staining viewed with polarised light. Images show collagen distribution in A: control, B: Cd, C: Hg and D: Cd + Hg groups. Arrows indicating the distribution of collagen type III (yellow – green birefringence) and type I fibres (orange – red birefringence) (Scale bars = 20 µm).

Figures 3 A - D are light micrographs representing the bronchiole structure of the control (Figure 3 A) and exposed groups (Figure 3 B - D). Figure 3 A shows the typical structure of a bronchiole with an intact epithelial lining (E) and a regular arrangement of smooth muscle (SM) surrounding the bronchiole. Figure 3 B and D (asterixs) show desquamation of the epithelium resulting in cellular debris within the bronchioles, and stratification of the bronchiole epithelium, (indicated by SE). Also, the smooth muscle surrounding the bronchioles in both Cd and the combination groups appears to have an irregular displacement. In the Hg exposed group (Figure 3 C), the infiltration of inflammatory cells was observed by the presence of bronchus associated lymphoid tissue (BALT) which was not observed in the control samples.

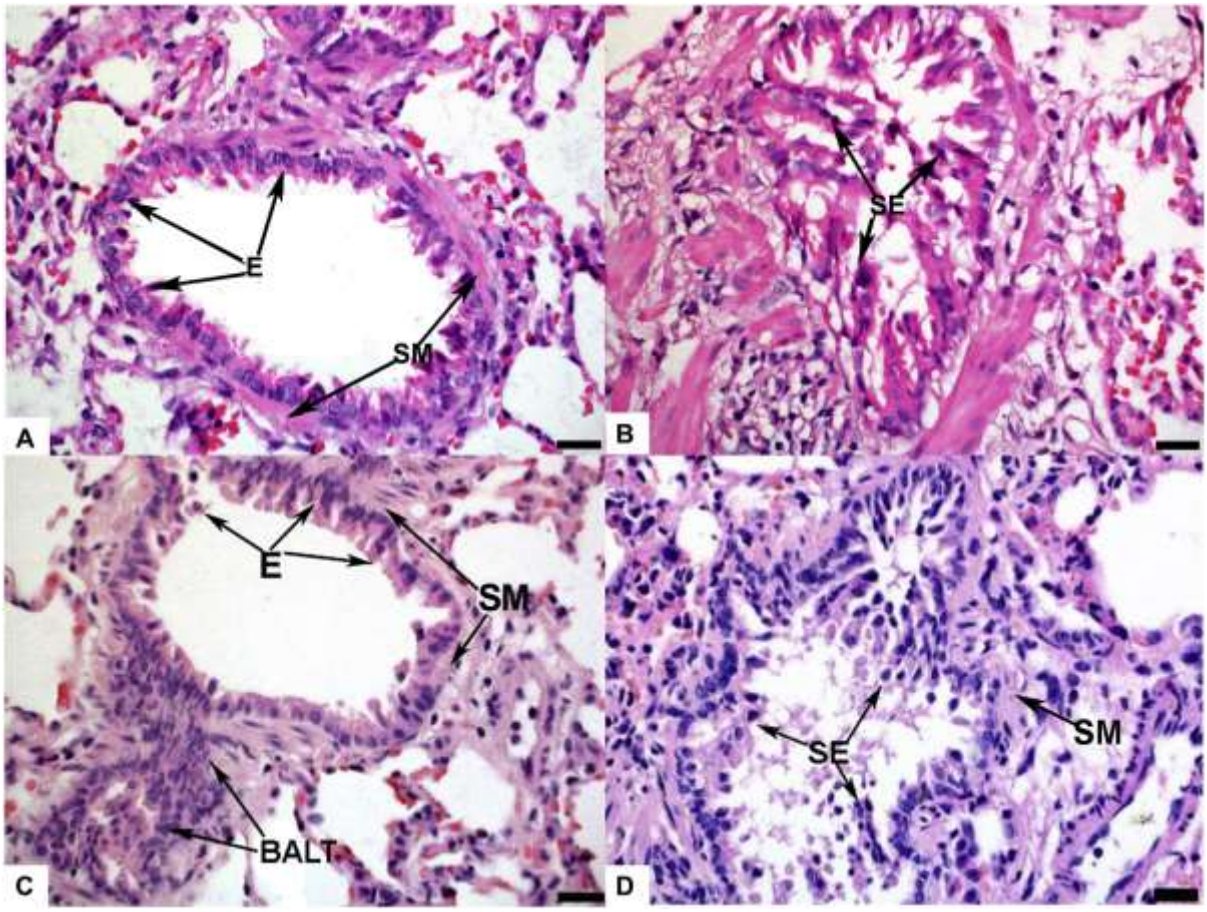

Figure 3: General structure of the bronchioles. H&E staining. A: Control; B: Cd; C: Hg; D: Cd + Hg. Labels: E: bronchial epithelium; SM: smooth muscle in the lamina propria; SE: stratification of epithelium; BALT: bronchus associated lymphoid tissue; *: desquamated epithelial cells (Scale bars = 20 µm).

Figures 4 A - D are light micrographs of the bronchiole structures stained with PR and viewed with polarised light. The bronchioles showed a prominent change of the collagen fibres between the control (Figure 4 A) and exposed (Figure 4 B - D) groups. As seen in Figure 4 A, the control has type III collagen fibres (green birefringence) that are arranged more loosely and thinner whereas Type I collagen fibres are more dense and thicker as observed in the

exposed groups shown in Figure 4 B - D with red and orange interwoven birefringence. The control (Figure 4 A) has an interwoven distribution of green and yellow collagen fibres. In the Hg and combination exposed groups, there was a decrease in type III collagen (green - yellow birefringence) and increase in type I collagen (orange – red birefringence) along the epithelial lumen (thin white arrow) and the epithelium (thick white arrow).

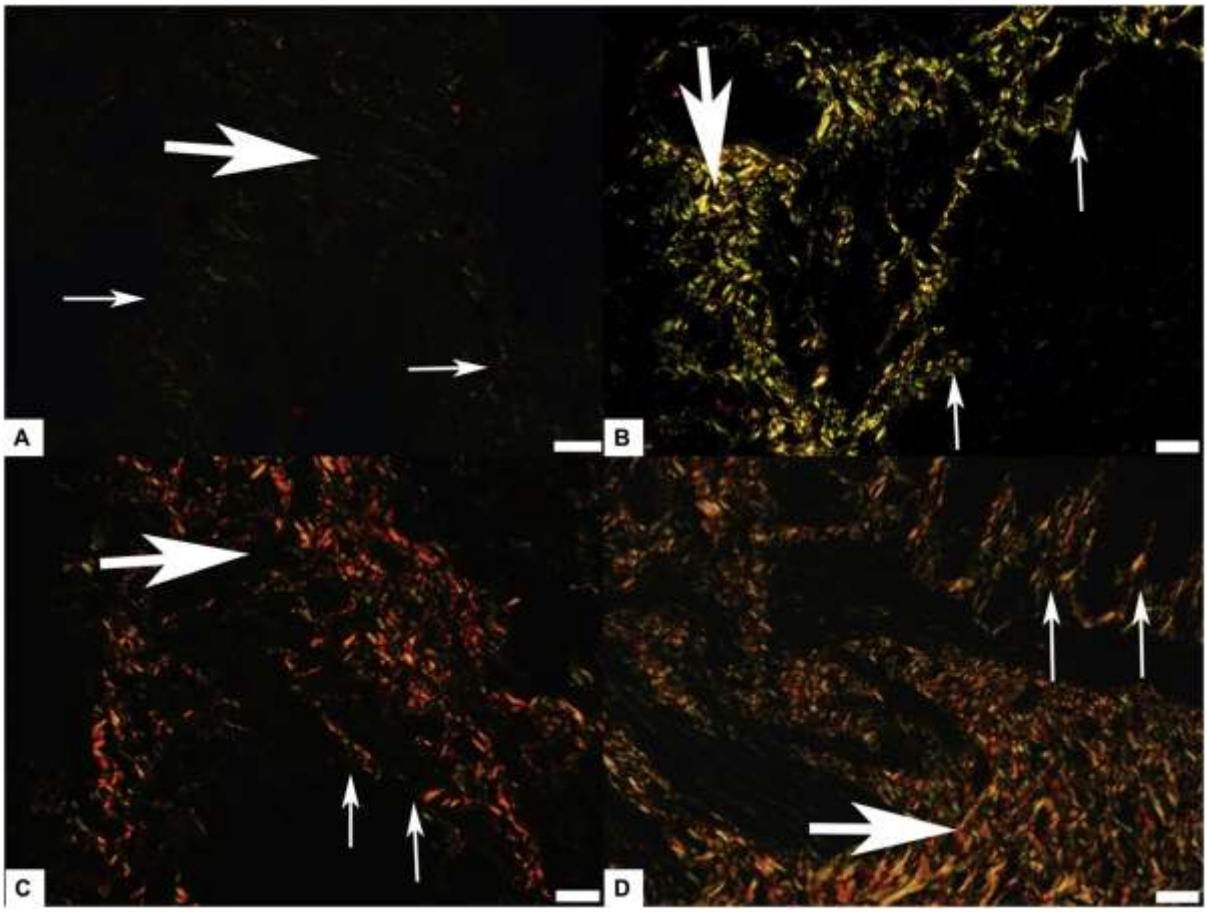

Figure 4: Collagen distribution in the bronchioles. PR staining and viewed with polarized light. A: Control; B: Cd; C: Hg; D: Cd + Hg. Thin white arrows indicate an increase in fibre thickness associated with the bronchioles mucosa and thick arrows indicates an increase in the submucosa. Collagen type III (yellow – green birefringence) and type I fibres (orange – red birefringence) (Scale bars = 20 µm).

Figure 5 A - D focuses on the arrangement of elastic fibres in the bronchioles of control compared to the exposed groups. The elastic fibres in the exposed groups (Figure 5 B - D) appear irregular and not continuous with the basement membrane of the epithelial lining of the bronchioles, when compared to the control (Figure 5 A). Smooth muscle stains pink and increased amounts and altered distribution of smooth muscle is observed in Figure 5 B - D.

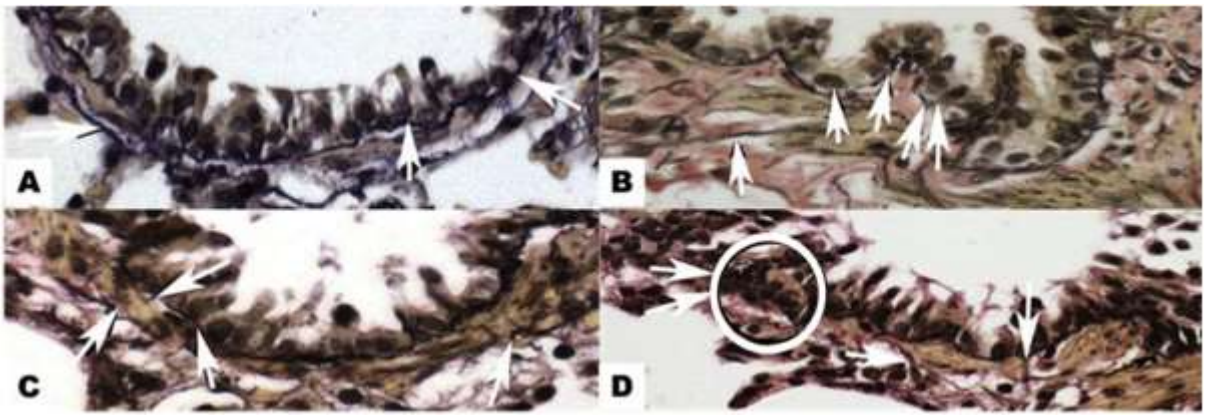

Figure 5: Mucosa of the bronchioles. VvG staining A: Control; B: Cd; C: Hg; D: Cd + Hg. Elastic fibres are indicated by the white arrows and smooth muscle stains pink. Circled: BALT (Scale bars = 20 µm).

Figure 6 A - D represents the ultrastructural features of the bronchioles in control (Figure 6 A) and metal exposed groups (Figure 6 B - D). Collagen fibres were observed in the control group, indicated by the black arrow in Figure 6 A. More prominent and densely arranged collagen fibril bundles were observed in the heavy metal exposed groups (Figure 6 B – D, black arrow) located in between the elastin fibres (arrowhead). Prominent elastin bundles (white arrowheads) were evident in the exposed groups. The collagen distribution is prominent in both single exposure groups Cd (Figure 6 B) and Hg (Figure 6 C) compared to the control (Figure 6 A). Collagen bundles appear most densely arranged and coiled in the Cd group, while the Hg group presented with additional fragmented elastin. In the Cd + Hg group (Figure 6 D); both collagen and elastin are more noticeable.

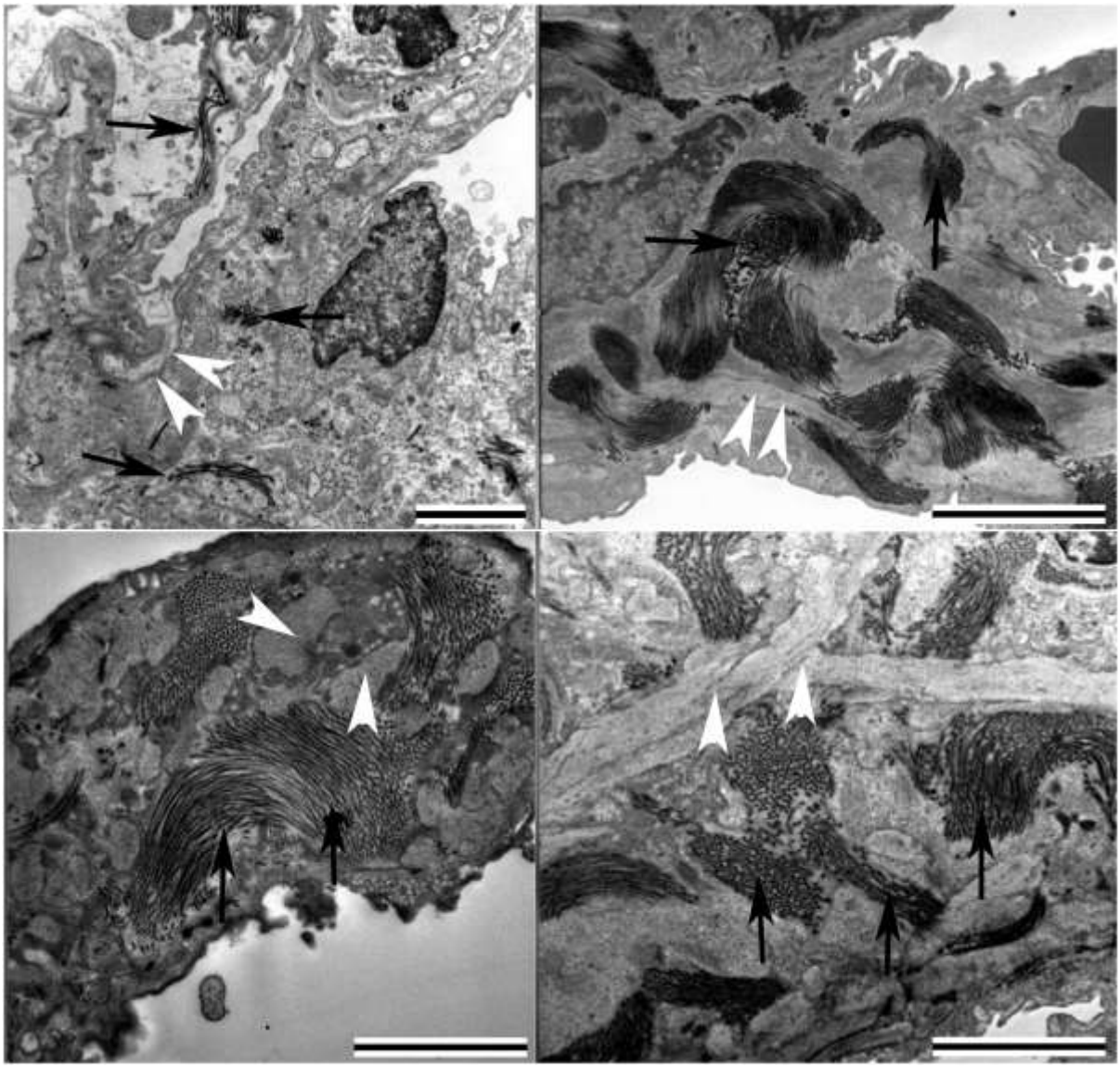

Figure 6: Transmission electron micrographs of bronchioles A: Control; B: Cd; C: Hg; D: Cd + Hg. Black arrows: collagen fibres; white arrowheads: elastin bundles (Scale bars = 2 µm).

4. Discussion

To determine the effects of oral exposure to heavy metals, changes in the functioning and morphology of the liver and kidneys are usually investigated (Kenston *et al*., 2018). In the present study, the effect of oral exposure to Cd and Hg alone and combination at 1000 times the WHO acceptable water limits on lung tissue was evaluated. Changes to the structure of the lungs and bronchiole were determined and this included the alveoli, air-blood barrier morphology and the distribution of connective tissue; collagen and elastin.

In the lungs of exposed rats, the interalveolar spaces appeared thickened associated with an increase in the presence of RBC, which indicates endothelial damage that can adversely affect

the functioning of the air-blood barrier. Heavy metal induced oxidative stress causes membrane damage, which can lead to membrane destabilisation and disintegration (Stajn *et al*., 1997). Damage to the air-blood barrier and increase in permeability of the pulmonary epithelium leads to plasma protein extravasation (Valcheva-Kuzmanova *et al*., 2014) resulting in pulmonary oedema. Pneumocyte type II cells are vulnerable to oxidative stress and Hg induces type II epithelial cell damage via the oxidative stress associated mitochondrial cell death pathway (Lu *et al*., 2010). Shedding of the epithelial cells and cellular debris resulting in the obliteration of the bronchiolar lumen was observed in the lungs of rats exposed to Cd and Cd + Hg groups (Figure 3 B and D).

In the exposed rats, the smooth muscle in the bronchioles is irregularly displaced and BALT appears to be more prominent in exposed groups (Figure 3 C). Irregular displacement and smooth muscle accumulation are events also observed in the histopathology of asthma (Bai and Knight, 2005). Inflammatory cells are recruited into the tissue from the circulation when local defences systems fail. The influx of inflammatory cells into the interstitium and bronchoalveolar space, is considered and important factor in the progression of lung injury (Grommes and Soehnlein, 2011). Inflammatory cell infiltration, specifically mast cell infiltration has been linked to airway hyper responsiveness (Brightling *et al*., 2005). An increase in bronchial smooth muscle is associated with lung dysfunction in severe asthma (Bousquet and Jeffery, 2000; Kaminska *et al*., 2009). Smooth muscle itself is able to recruit inflammatory cells that participate in the inflammatory activation loop (Berger *et al*., 2003). Improper tissue repair and epithelial regeneration after injury can result in excessive fibroproliferation and inflammation in the sub-epithelial structures. This is often observed in obliterative bronchiolitis and injury to the bronchiolar epithelium (Barker *et al*., 2014). Exposure to Cd and Cd + Hg (Figure 3 B and D) also caused basement membrane detachment, resulting in bronchiole epithelium stratification and the presence of cellular debris in the lumen. These changes are consistent with histological changes observed in asthma and chronic bronchitis (Bai and Knight, 2005; Salvato, 1968).

Evaluation of the effects on collagen and elastic fibre distribution in the lungs of exposed rats showed an increased collagen deposition and differences in the type of collagen deposited in the interalveolar septa. For all rats exposed to metals there was an increase in collagen deposition, with collagen type I being the prominent type.

Elastic fibres in bronchioles are associated with the basement membrane and facilitates bronchial patency during respiration. Exposure to Cd, Hg and Cd + Hg (Figure 5 B - D) resulted in irregular elastic fibre distribution not continuous with the basement membrane. Changes in the distribution of elastic fibres are due to the elastic lamina being disrupted and delineated

from the bronchioles basement membrane (Harris *et al*., 2016) while increased presence of elastin which may be a consequence of changes to epithelial structure and/or increased fibrosis. Increased deposition and abnormal of collagen and elastin fibres was confirmed with TEM.

Airway remodelling is associated with an increase in collagen deposition, altered distribution of collagen, mucous gland hypertrophy, smooth muscle hyperplasia or hypertrophy; all contributing to long term irreversible changes, a fixed airway obstruction and severity of asthmatic disease (Begueret *et al*., 2007). The increased deposition and synthesis of a collagen type often results in structural abnormalities of the connective tissue. Increased synthesis of type I collagen, as is shown in Figure 4 B - D, is often associated with fibrosis (Arbi *et al.,* 2015). Interwoven red-orange birefringence indicative of collagen type I, which is associated with fibrosis, was observed for the Hg and Cd + Hg exposure groups.

While the bronchioles showed a prominent increase in type I collagen fibres in the exposed groups, irregular displacement of elastin fibres around the bronchioles, not being continuous with the basement membrane of the bronchiole compared to control, was observed. Transmission electron microscopy analysis showed an increase in collagen and elastin bundles of the exposed groups compared to control.

Damage to the elastic fibres can occur as a result of damage or inflammation. In asthma, elastic fibres show a thickened and patchy morphology as well as fibre tangling which may be the result of repair elicited by chronic inflammation. Elastosis in the airways and a gradual remodelling of the airways through reorientation of fibres has also been observed in chronic lung disease (Bergeron *et al*., 2009; Kumar, 2001; Yang *et al*., 2016). Alveolar wall destruction and reduced elastic recoil due to the destruction of elastin and increase deposition of collagen are characteristic features of emphysema (Zhou *et al*., 2018).

Effects of Hg on the lungs have largely been described as a result of exposure to Hg vapour via inhalation. Occupational or accidental exposure to Hg vapour has been shown to lead to acute respiratory failure (Smiechowicz *et al*., 2017; Rowens *et al*., 1991; Asano *et al*., 2000; Moromisato *et al*., 1994; Lim *et al*., 1998) pulmonary oedema and acute interstitial pulmonary fibrosis (Jaeger *et al*., 1979). Similar to the present study, Celikoglu *et al*., (2015) observed in rats that were daily orally exposed to 1mg/kg for 28 days, Hg caused alveolar oedema, haemorrhage, interalveolar thickening, inflammatory cell infiltration and fibrosis.

Collagen found within smooth muscle affects muscle contractility, as was observed in collagen deposition in detrusor muscle and urinary retention (Bellucci *et al*., 2017). Severe and non – severe asthma patients present with thickened airway smooth muscle and thicker extracellular matrix (ECM) deposition (Begueret *et al*., 2007). Smooth muscle activation in the airways

would cause excessive bronchoconstriction, and increased muscle mass would further promote this effect. The response of excessive bronchoconstriction is linked directly to underlying inflammation. An increase in transforming growth factor beta (TGF-β) has been observed in asthmatic airways (Redington *et al*., 1997; Vignola *et al*., 1997) and TGF-β is known to induce fibronectin and collagen type I deposition in bronchial smooth muscle cells through connective tissue growth dependant and independent pathways (Johnson *et al*., 2006). Bronchial smooth muscle cells are therefore able to control their own environment (Bara *et al*., 2010). Changes of elastin were shown to cause limitations to the airflow through the airways and into the alveoli (Black *et al*., 2008). In the present study electron microscopy revealed the increased abundance of elastin and collagen bundles in the bronchioles (Figure 4 and 6) indicating the possible contribution of Cd and/or Hg to the development of asthma.

Heavy metals induce oxidative stress which has been implicated in the fibrogenesis through the induction of fibrogenic cytokines such as TGF - β, connective tissue growth factor (CTGF), and platelet-derived growth factor (PDGF) (Shroff *et al*., 2011). The cytokines contribute to an increase in collagen synthesis and deposition by stimulating the differentiation of fibroblasts from mesenchymal, epithelial and endothelial cells (Barker *et al*., 2014). High collagen III to collagen I ratio is observed in early fibrosis while a low collagen III to collagen I ratio is observed in late fibrosis, associated with idiopathic pulmonary fibrosis. Furthermore idiopathic pulmonary fibrosis is a self-perpetuating fibrosis through a positive feedback mechanism (Murtha *et al*., 2017).

The involvement of inflammation and inflammatory mechanisms in promoting pulmonary fibrosis has been well described (Kolahian *et al*., 2016). Recently a new pathway for Cd-induced collagen stimulation and further matrix stiffening has been described involving Yes-associated protein 1 (YAP1) activation (Li *et al*., 2017), whose function is to mediate TGF-β induced signalling in the lung (Pefani *et al*., 2016). Activation of YAP1 causes matrix stiffening, which further promotes nuclear localisation of YAP1, so that it moves from the cytoplasm to the nucleus where it binds to Smad2/3 and activates fibrosis mediated transcription factors (Li *et al*., 2017). Lysyl oxidase has been found to be a target of cigarette smoke of which Cd is a major component (Li *et al*., 2011). Cd down regulates the expression of lysyl oxidase at mRNA, protein and catalytic levels in lung cells, both *in vitro* and *in vivo*. An inhibition of lysyl oxidase which is Cu dependant and catalyses the cross linking of collagen and elastin, stabilising the ECM. The limitation of Cu cofactor by Cd accelerates collagen and elastin damage. These changes are important in the development of emphysema (Zhao *et al*., 2006). Low dose Cd induces peribronchiolar fibrosis characterised by luminal loss and remodelling in small airways and (Li *et al*., 2017). Peribronchiolar fibrosis can occur before the onset of emphysema (Hogg *et al*., 2004) and may be present together with alveolar wall loss (Lang *et al*., 1994; Vlahovic

et al., 1999). Cd has been suggested to be attributed to pulmonary emphysema through altered redox balance and macrophage dysfunction (Ganguly *et al*., 2018) and Hg has been shown to cause oxidative stress in lungs (Ansar and Iqbal, 2015). These hypothesised mechanisms are summarised in Figure 7.

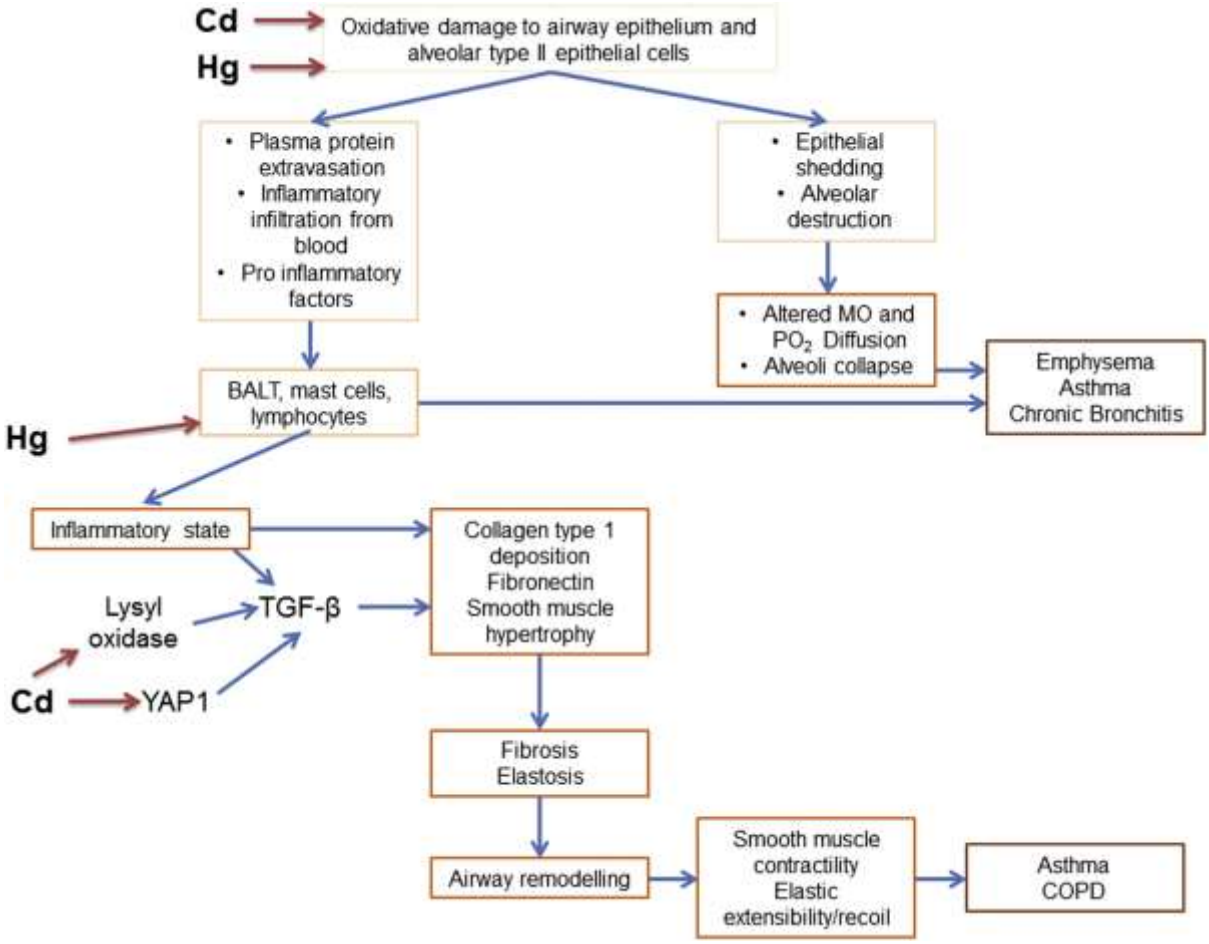

Figure 7: Flow diagram of the hypothesised mode of action of Cd and Hg on lung tissue, contributing to lung pathologies associated with asthma, chronic bronchitis, COPD and pulmonary fibrosis.

Changes to lung function is often reported to be due to heavy metals such as Cd and Hg being air pollutants. However, increasing exposure to water contaminated with Cd and Hg, may via a similar pathway of oxidative stress, alter the structure of lung tissue leading to the development of associated disease especially if exposure is to metals as part of mixtures as is reported for Cd and Hg in the present study. The reported ability of Hg to stimulate the immune system (Weigand *et al*., 2015) could explain the elevated fibrosis and elastin damage and ECM remodelling in the Cd and Hg exposure group. Along with the fibrotic induction with oxidative stress caused by both metals individually, Hg has an additional pro-inflammatory effect, which may contribute to the elevated damage observed in the combination group.

5. Conclusion

This study showed that environmental exposure to heavy metals Cd and Hg in water results in fibrosis associated with an increase in type I collagen synthesis in the airways and alveoli. Additional irregular smooth muscle arrangement and destruction of elastic fibres in the bronchiole further also contributes to pathology. In the lungs, alveolar type II epithelial cell damage as a result of an increased oxidative environment, initiates an inflammatory reaction and subsequent fibrosis, which is further amplified by the metals ability to directly contribute to the inflammatory and fibrotic process. The clinical implications of exposure to water contaminated with Cd and Hg is an increased risk for the development of asthma, chronic bronchitis and potentially COPD.

Acknowledgements

The authors wish to thank the National Research Foundation for the funding of this study. (Grant number: 92768)

References

Ansar, S., and Iqbal, M., 2015. Effect of dietary antioxidant on mercuric chloride induced lung toxicity and oxidative stress. *Toxin Rev.*, *34*(4):168-172.

Arbi, S., Eksteen, E.C., Oberholzer, H.M., *et al*, 2015. Premature collagen fibril formation, fibroblast-mast cell interaction and mast cell mediated phagocytosis of collagen in keloids. *Ultrastruct Pathol*, 1-9.

Asano, S., Eto, K., Kurisaki, E., *et al*, 2000. Acute inorganic mercury vapor inhalation poisoning*. Pathol Int.* 50(3):169–174.

Awofolu, O.R., Mbolekwa, Z., Mtshemla, V., *et al.,* 2005. Levels of trace metals in water and sediment from Tyume River and its effects on an irrigated farmland. *AJOL*. 331(1):87-94.

Bai, T.R. and Knight, D.A., 2005. Structural changes in the airways in asthma: observations and consequences. *Clin Sci*. 108(6): 463-477.

Bara, I., Ozier, A., de Lara, T., *et al*., 2010. Pathophysiology of bronchial smooth muscle remodelling in asthma. *European respiratory journal* 36: 1174-1184

Barker, A.F., Bergeron, A., Rom, W.N., Hertz, M.I., 2014. Obliterative bronchiolitis. *N Engl J Med*. 370:1820-1828

Begueret, H., Berger, P., Vernejoux, J.M., *et al.,* 2007. Inflammation of bronchial smooth muscle in allergic asthma. *Thorax*, *62*(1): 8-15.

Bellucci, C.H., Ribeiro, W.D.O., Hemerly, T.S., *et al.,* 2017. Increased detrusor collagen is associated with detrusor overactivity and decreased bladder compliance in men with benign prostatic obstruction. *Prostate Int. 5*(2): 70-74.

Berger, P., Girodet, P. O., Begueret, H., *et al*., 2003. Tryptase-stimulated human airway smooth muscle cells induce cytokine synthesis and mast cell chemotaxis. *FASEB J*. 10.1096/fj.03-0041

Bergeron, C., Al-Ramli, W., Hamid, Q., 2009. Remodeling in asthma. *Proc. Am. Thorac. Soc*. 6:301–305.

Bertin, G., Averbeck, D. 2006. Cadmium: Cellular effects, modifications of biomolecules, modulation of DNA repair and genotoxic consequences (a review). *Biochimi.* 88: 1549-1559

Black, P. N., Ching, P. S., Beaumont, B., *et al*., 2008. Changes in elastic fibres in the small airways and alveoli in COPD. *Eur Respir J*. 31: 998-1004

Borges, L.F., Gutierrez, P.S., Marana Sebastia, H.R.C., *et al.,* 2007. Picro picrosirius-polarization staining method as and efficient histopathological tool for collagenolysis detection in vesical prolapse lesions. *Micron.* 38: 580-583.

Bousquet, J., Jeffery, P., 2000. Asthma from bronchoconstriction to airways inflammation and remodeling. *Am J Respir Crit Care Med*. 161:1720–1745

Brightling, C.E., Ammit, A.J., Kaur, D., *et al*., 2005. The CXCL10/CXCR3 Axis mediates human lung mast cell migration to asthmatic airway smooth muscle. *Am J Respir Crit Care Med.* 171:1103–1108.

Celikoglu, E., Aslanturk, A. and Kalender, Y., 2015. Vitamin E and sodium selenite against mercuric chloride induced lung toxicity in the rats. *Braz Arch Technol.* 58(4):587-594.

Ganguly, K., Levänen, B., Palmberg, L., Åkesson, A. and Lindén, A., 2018. Cadmium in tobacco smokers: a neglected link to lung disease? *Eur Respir Rev*. *27*(147): 170-179.

Grommes. J., Soehnlein, O., 2011. Contribution of neutrophils to acute lung injury. *Mol Med.* 17:293-307

Harris, W.T., Boyd, J.T., McPhail, G.L., *et al.*, 2016. Constrictive bronchiolitis in adolescents with cystic fibrosis with refractory pulmonary decline. *All Annals ATS*. 13(12): 1-34.

Hogg, J.C., Chu, F., Utokaparch, S., et al., 2004. The nature of small-airway obstruction in chronic obstructive pulmonary disease. *N Engl J Med* 350:2645–2653

Huff, J., Lunn, R.M., Waalkes, M.P., *et al*., 2007. Cadmium-induced cancers in animals and in humans. *Int J Occup Environ Health* 13(2):202–212.

Jaeger, A., Tempe, J.D., Haegy, J.M., Leroy, M., Porte, A. and Mantz, J.M., 1979. Accidental acute mercury vapor poisoning. *Vet Hum Toxicol*. *21*: 62-63.

Jarup, L. Hazards of heavy metal contamination. 2003. British medical bulletin. 68(1): 167-182

Johnson, P.R., Burgess, J.K., Ge, Q., *et al.,* 2006. Connective tissue growth factor induces extracellular matrix in asthmatic airway smooth muscle. *Am J Respir Crit Care Med*. 173: 32–41.

Kaminska, M., Foley, S., Maghni, K., *et al,* 2009. Airway remodeling in subjects with severe asthma with or without chronic persistent airflow obstruction. *J Allergy Clin Immunol*. 124(1): 45–51.

Kenston, S. S. F., Su, H., Li, Z., *et al*., 2018. The systemic toxicity of heavy metal mixtures in rats. *Toxicol Res*. 7: 396-407

Kolahian, S., Fernandez, I.E., Eickelberg, O., Hartl, D., 2016. Immune mechanisms in pulmonary fibrosis. *Am J Respir Cell Mol Biol.* 55: 309–322.

Kumar, R.K., 2001. Understanding airway wall remodeling in asthma: a basis for improvements in therapy. *Pharmacol Ther.* 91: 93–104.

Lang, M.R., Fiaux, G.W., Gillooly, M., *et al.,* 1994. Collagen content of alveolar wall tissue in emphysematous and non-emphysematous lungs. *Thorax.* 49: 319–326.

Leem, A.Y., Kim, S.K., Chang, J., *et al*., 2015. Relationship between blood levels of heavy metals and lung function based on the Korean National Health and Nutrition Examination Survey IV–V. *Int J Chron Obstruct Pulmon Dis*. 10: 1559–1570.

Li, F.J., Surolia, R., Li, H., Wang, Z., *et al.,* 2017. Low-dose cadmium exposure induces peribronchiolar fibrosis through site-specific phosphorylation of vimentin. *Am J Physiol Lung Cell Mol Physio 313*(1):80-91.

Li, W., Zhou, J., Chen, L., Luo, Z. and Zhao, Y., 2011. Lysyl oxidase, a critical intra-and extra-cellular target in the lung for cigarette smoke pathogenesis. *Int J Environ Res Public Health*. *8*(1): 161-184.

Lim, H.E., Shim, J.J., Lee, S.Y., *et al.,* 1998. Mercury inhalation poisoning and acute lung injury. *Korean J Intern Med 1998*. 13(2): 127–130.

Lu, T.H., Chen, C.H., Lee, M.J., *et al.,* 2010. Methylmercury chloride induces alveolar type II epithelial cell damage through an oxidative stress-related mitochondrial cell death pathway. *Toxicol Lett*. *194*(3): 70-78.

Luo, H., Xu, P., Roane, T.M., *et al.*, 2011. Microbial desalination cells for improved performance in wastewater treatment, electricity production, and desalination. *Bioresour Technol*. 105: 60-66.

Mamuya, S.H.D., Bratveit, M., Mashalla, Y., and Moen, B.E., 2007. High prevalence of respiratory symptoms among workers in the development section of a manually operated coal mine in a developing country: A cross sectional study. *BMC Public Health*. 2458: 7-17.

Martin, S., Griswold, W., 2009. Human health effects of heavy metals. *Environ Sci Technol Briefs Citizens*.15:1–6.

McCarthy, T.S., 2011. The impact of acid mine drainage in South Africa. *SA J Sci.* 107(5), 5-6.

Moromisato, D.Y., Anas, N.G. and Goodman, G., 1994. Mercury inhalation poisoning and acute lung injury in a child. Use of high frequency oscillatory ventilation. *Chest.* 105(2), 613–615.

Murtha, L.A., Schuliga, M.J., Mabotuwana, N.S., Hardy, S.A., Waters, D.W., Burgess, J.K., Knight, D.A. and Boyle, A.J., 2017. The processes and mechanisms of cardiac and pulmonary fibrosis. *Front Physiol. 8*: 777 – 789.

Naicker, K., Cukrowska, E., and McCartht, T.S., 2003. Acid mine drainage arising from gold mining activity in Johannesburg, South Africa and environs. *Environ Pollut*. 122(1): 29-40.

Nawrot, T.S., Staessen, J.A., Roels, H. A., *et al.,* 2010. Cadmium exposure in the population: from health risks to strategies of prevention. *Biometals* 23(5): 769-782

Onyido, I., Norris, A. R., Buncel, E. 2004. Biomolecule−Mercury Interactions: Modalities of DNA Base−Mercury Binding Mechanisms. Remediation Strategies. *Chem Rev* 104(12): 5911-5930

Pefani, D.E., Pankova, D., Abraham, A.G., *et al.,* 2016. TGF-β targets the Hippo pathway scaffold RASSF1A to facilitate YAP/SMAD2 nuclear translocation. *Mol Cell.* 63: 156–166.

Reagan-Shaw, S., Nihal, M., Ahmad, N., 2008. Dose translation from animal to human studies revisited. *The FASEB J*. 22(3): 659-661.

Redington, A.E., Madden, J., Frew, A.J., *et al.*, 1997. Transforming growth factor-beta 1 in asthma. Measurement in bronchoalveolar lavage fluid. *Am J Respir Crit Care Med.* 156: 642–647.

Rehman, K., Fatima, F., Waheed, I., *et al.,* 2018. Prevalence of exposure of heavy metals and their impact on health consequences. *J Cell Biochem*. 119:157-184.

Rowens, B., Guerrero-Betancourt, D., Gottlieb, C.A*., et al*., 1991. Respiratory failure and death following acute inhalation of mercury vapor. A clinical and histologic perspective. *Chest.* 99(1): 185–190.

Salvato, G. 1968. Some histological changes in chronic bronchitis and asthma. *Thorax*. 23(2); 168-172.

Shroff, A., Mamalis, A., and Jagdeo, J., 2014. Oxidative stress and skin fibrosis. *Curr Pathobiol Rep.* 2, 257-267.

Smiechowicz, J., Skoczynska, A., Nieckula-Szwarc, A., *et al*., 2017. Occupational mercury vapour poisoning with a respiratory failure, pneumomediastinum and severe quadriparesis. *SAGE open medical case reports*. 5: 1-4

Stajn, A., Ziki, R.V., Ognjanovic, B., *et al.,* 1997. Effect of cadmium and selenium on the antioxidant defence system in rat kidneys*. Comp Biochem Physiol*. 2: 167-172.

Valcheva-Kuzmanova, S., Stavreva, G., Dancheva, V., *et al.,* 2014. Effect of *Aronia melanocarpa* fruit juice on amiodarone-induced pneumotoxicity in rats. *Pharmacogn Mag.* 10: 132-140.

Velindala, S., Gaikwad, P., Ella, K.K.R., Bhorgonde, K.D., Hunsingi, P., Anop, K., 2014. Histochemical analysis of polarizing colours of collagen using Picro Sirius red staining in oral submucous fibrosis. *J Oral Health*. 6(1): 33-38.

Venter, C., Oberholzer, H.M., Cummings, F.R., *et al.*, 2017. Effects of metals cadmium and chromium alone and in combination on the liver and kidney tissue of male Spraque-Dawley rats: An ultrastructural and electron-energy-loss spectroscopy investigation. *Microsc Res Tech.* 80(8): 878-888.

Vignola, A.M., Chanez, P., Chiappara, G., *et al.*, 1997. Transforming growth factor-β expression in mucosal biopsies in asthma and chronic bronchitis. *Am J Respir Crit Care Med.* 156: 591–599.

Vlahovic, G., Russell, M.L., Mercer, R.R., Crapo, J.D.,1999. Cellular and connective tissue changes in alveolar septal walls in emphysema. *Am J Respir Crit Care Med.* 160, 2086–2092.

Weigand, K.L., Reno, J.L. and Rowley, B.M., 2015. Low-level mercury causes inappropriate activation in T and B lymphocytes in the absence of antigen stimulation. *J Arkansas Acad Sci*. *69*(1): 116-123.

WHO (World Health Organisation), 2000. Cadmium: Air Quality Guidelines, 2nd. World Health Organisation, Regional Office for Europe, Copenhagen, Denmark. Chapter 6.3.

Yang, L., Li, J., Mo, H., Pidaparti, R.M., Witten, T.M., 2016. Possible role of collagen reorientation during airway remodeling on mucosal folding. *J. Eng. Math.* 96: 37–56.

Zhao, Y., Gao, S., Chou, I.N., *et al.,* 2006. Inhibition of the expression of lysyl oxidase and its substrates in cadmium-resistant rat fetal lung fibroblasts. *Toxicol Sci*. *90*(2): 478-489.

Zhou, Y., Horowitz, J.C., Naba, A., *et al.,* 2018. Extracellular matrix in lung development, homeostasis and disease. *Matrix Biol.* 73: 77- 104.

Zhu, H., Jia, Y., Cao, H., *et al.,* 2014. Biochemical and histopathological effects of subchronic oral exposure of rats to a mixture of five toxic elements. *Food Chem Toxicol*. 71: 166-175.